



## Investigation of the Effect of Copper Nanoparticle Deposition on Low-Carbon Steel using Physical Vapor Deposition for Solar Cooling Application

Mohd Anas Mohd Sabri<sup>1,2,\*</sup>, Mohamed Sadeq Jaffer Albaaj<sup>1</sup>, Meor Iqram Meor Ahmad<sup>1,2</sup>, Wan Aizon Wan Ghopa<sup>1,2</sup>, Siddig A. Omer<sup>3</sup>

- <sup>1</sup> Department of Mechanical & Manufacturing Engineering, Faculty of Engineering & Built Environment, Universiti Kebangsaan Malaysia, 43600 Bangi, Selangor, Malaysia  
<sup>2</sup> Centre for Automotive Research (CAR), Faculty of Engineering & Built Environment, Universiti Kebangsaan Malaysia, 43600 Bangi, Selangor, Malaysia  
<sup>3</sup> Institute of Sustainable Energy Technology, Department of Architecture and Built Environment, Faculty of Engineering, University of Nottingham, Nottingham NG7 2RD, United Kingdom

### ARTICLE INFO

#### Article history:

Received 8 August 2024  
Received in revised form 11 September 2024  
Accepted 19 October 2024  
Available online 30 November 2024

#### Keywords:

Nanomaterials; Cu-NP; nanoparticle coating

### ABSTRACT

The use of nanomaterials in solar cooling applications has gained significant attention in recent years. This study aimed to increase thermal conductivity by depositing copper nanoparticles (Cu-NP) on low-carbon steel using thermal evaporation and a physical vapor deposition (PVD) method. Low-carbon steel was selected as the substrate due to its wide use in thermal applications and strong absorption properties. The presence of Cu-NP on the surface was analysed using XRD and thermal characteristics of the thin layer were determined using Thermal Constant Analyzer (TCA) and Transient Plane Source (TPS) measurements. Results showed that the copper nanoparticle coating sample on the carbon steel substrate had better heat emission and absorption compared to the carbon steel alone. It also shows some improvement of around 1% in the thermal conductivity results. This study demonstrates the potential of using Cu-NP deposited on low-carbon steel as a promising material for solar thermal/cooling applications.

## 1. Introduction

The increasing demand for clean and renewable energy has sparked interest among scientists in search of new energy sources [1]. Solar energy is a crucial aspect of this research due to its affordability, purity and absence of hazardous emissions and it has the potential to be converted into other forms of energy [2]. The absorber surface of a solar thermal collector plays a vital role in absorbing sunlight and converting it into heat [3]. To be effective, the absorber surface must effectively absorb as much ultraviolet-visible (UV-Vis) wavelength range light as possible and emit a

\* Corresponding author.

E-mail address: [anasms@ukm.edu.my](mailto:anasms@ukm.edu.my)

<https://doi.org/10.37934/armne.27.1.100111>

minimal amount of infrared (IR) light [4]. Additionally, thermal conductivity is a crucial factor in thermal applications, particularly in absorber surfaces and has drawn attention from researchers in this field [5]. In recent years, the introduction of nanoparticles in enhancing the capabilities of solar collector has become crucial. The use of nanoparticles in solar collectors has garnered significant interest due to their potential to enhance thermal performance and efficiency. Carbon Nanotubes (CNTs), particularly single-wall carbon nanotubes (SWCNTs), have been shown to enhance the heat transfer coefficient and reduce entropy generation in flat plate solar collectors. Their addition increases heat flux on the absorber plate, although it incurs a slight penalty in pumping power [6]. Hybrid nanoparticles, such as MWCNT/SiC (multi-wall carbon nanotube/silicon carbide), have been studied for their enhanced photothermal conversion performance in direct absorption solar collectors. These hybrid nanofluids exhibit superior thermal conductivity and stability, making them effective for solar applications [7]. Meanwhile, Employing and adding the aluminium oxide nanomaterial into the ETSC system contributed to several benefits and significant advantages. Using  $Al_2O_3$  enhanced thermal efficiency, increased the temperature of the outlet collector, improved the rate of heat flux of the pipes, the tube inside the collector, heat transfer of the hot water storage tank and raised the temperature gradient [8].

The use of Physical Vapour Deposition (PVD) technology can produce various types of coatings, including gradient coatings, metastable coatings, multilayer coatings, multicomponent coatings and superlattice coatings. Among these, multilayer coating seems to hold the most potential for meeting complex wear conditions, as it offers a multifunctional character, medium residual stresses, strong adhesion to metallic substrates, proper hardness, low friction coefficients and a desirable toughness ratio [9]. Additionally, this concept enables the use of metastable and multicomponent materials in a graded multilayer arrangement, providing a platform for the simultaneous implementation of different layer ideas and allowing for the tuning of characteristics and performance through layer-by-layer adjustments in material selection, volume modification and composition. Furthermore, studies have demonstrated that nanoparticles can significantly enhance the thermal absorption efficiency of various materials, as well as increase the corrosion resistance of some coatings [10-16].

Due to increasing energy demand in various industries, the exploration of natural energy resources has become a crucial area of study [17]. The sun is one of the most abundant natural energy sources and thus, researchers have focused on harnessing its energy. Solar energy is cost-effective, clean and environmentally friendly with minimal harmful emissions [18]. The absorber surface, a crucial component of the solar collector system, is responsible for absorbing sunlight and converting it into heat [19]. An efficient absorber surface must maximize absorption in the ultraviolet-visible wavelength while minimizing emission in the infrared or near-infrared region [3,20]. Low carbon steel has garnered considerable attention as a material for solar thermal systems, thanks to its favourable properties and cost-effectiveness. With its low carbon content and advantageous mechanical characteristics, low carbon steel presents an economical choice for absorber plates and heat exchangers in solar thermal applications [21]. Despite its many advantages, it is essential to acknowledge that low carbon steel may have lower thermal efficiency compared to some advanced materials, which remains a limitation [22]. Therefore, the aim of this paper is to study the performance of low carbon steel used in solar technology applications by applying a deposition of copper nanoparticles (Cu-NP) layer via the PVD method.

## **2. Methodology**

Figure 1 shows the experimental setup used to prepare a low carbon steel base metal coating with nano additives to enhance its thermal properties, such as conductivity, specific heat values and

thermal diffusion of the thin film. From this figure, we can observe five major activities involved: sample preparation, Physical Vapour Deposition (PVD) method on the sample, X-ray diffraction (XRD) analysis, Scanning Electron Microscopy (SEM) and lastly, thermal constant analysis using Transient Plane Source (TPS).

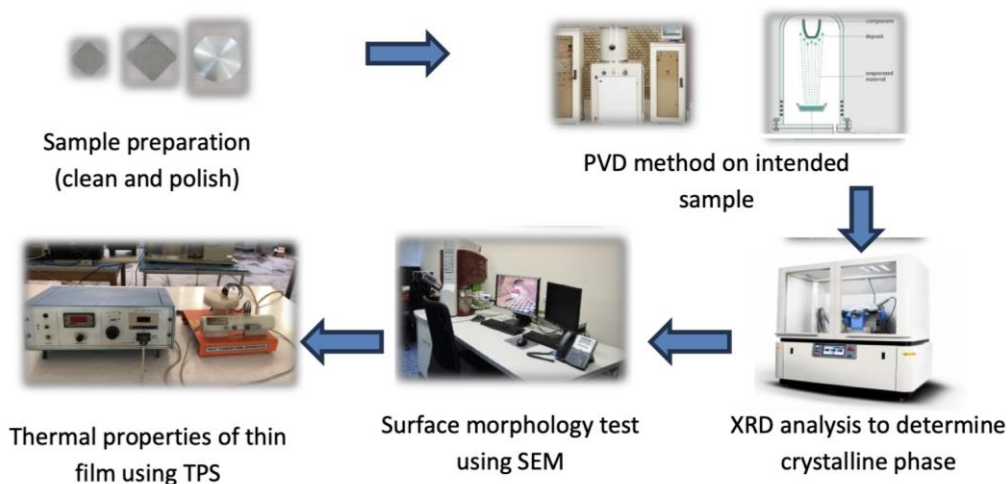


**Fig. 1.** Schematic diagram of low carbon steel deposited with Cu-NP experiment

Meanwhile, the entire process flow of the experimental procedure can be seen in Figure 2.

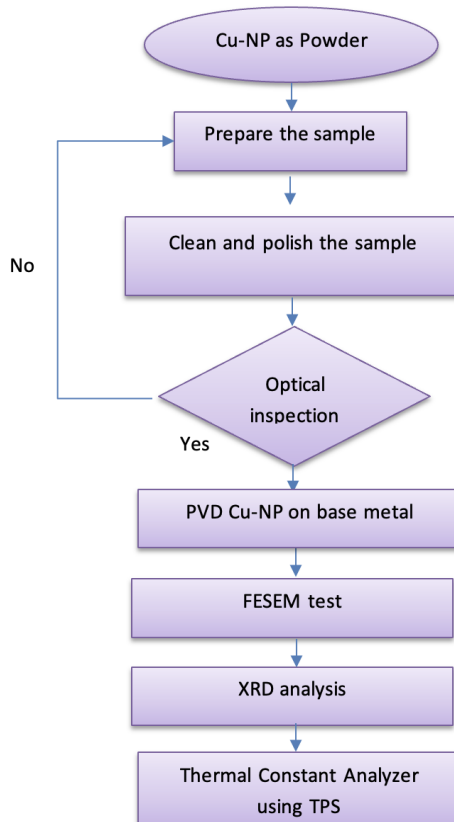


**Fig. 2.** The flow chart of low carbon deposited with Cu-NP process

## 2.1 Material

In the study, low carbon steel was selected as the base metal. Low carbon steel was selected as the base metal due to its versatile uses and heat absorption ability. The microstructure was analysed using a Spectrum test with the PMI-Master Pro Oxford Instruments tester. The specifications of the Copper Nano Particles (Cu-NP) to be used in the experiment are presented in Table 1.

**Table 1**  
 Specifications for Cu-NP

Property	The value	Units
Average particle diameter	30	nm
Purity	99.9	%
Specific surface area	15	M <sup>2</sup> /g
Density	8.9	g/cm <sup>3</sup>
Volume Density	0.2	g/cm <sup>3</sup>
Crystal form	Sphere	N/A
Colour	Brown	N/A

Meanwhile, Table 2 shows the results of the test conducted on the selected low carbon steel, where three tests were performed and the values were averaged to obtain the best results.

**Table 2**  
 Composition (%) results for the low carbon steel specimen

Specimen	Fe	C	Si	Mn	Cr	Mo	Ni	Al
1	99.5	0.0780	0.0050	0.350	0.0372	0.0040	0.0050	0.0020
2	99.5	0.0812	0.0050	0.335	0.0251	0.0040	0.0050	0.0020
3	99.5	0.0608	0.0050	0.366	0.0426	0.0040	0.0050	0.0020
Ave	99.5	0.0733	0.0050	0.350	0.0349	0.0040	0.0050	0.0020
Specimen	Co	Cu	Nb	Ti	V	W	Pd	Zr
1	0.0020	0.0085	0.0030	0.0010	0.0020	0.0250	0.0150	0.0030
2	0.0020	0.0086	0.0030	0.0010	0.0020	0.0250	0.0150	0.0030
3	0.0020	0.0051	0.0030	0.0010	0.0020	0.0250	0.0150	0.0030
Ave	0.0020	0.0074	0.0030	0.0010	0.0020	0.0250	0.0150	0.0030

## 2.2 Preparation of Substrate

The specimens used for the experimental tests were made of low carbon steel and were cut into square sizes. The samples were cut using a laser cutter machine to preserve the properties of the metal. Each sample has a thickness around 4.77 mm was cut to 20x20 mm and then cleaned and polished using a polishing machine. The substrate sample can be seen in Figure 3.

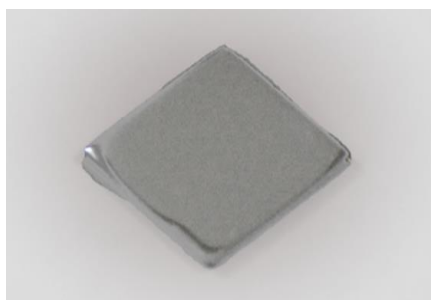


**Fig. 3.** The samples used for the experiment

### 2.3 Thin Film Preparation Procedure with PVD

As previously mentioned, PVD processes involve the vaporization of materials into atoms or molecules from a solid or liquid source, which are then transported to the substrate as a vapor through a vacuum or plasma environment and deposited as a thin film. PVD methods are typically used to deposit films with a thickness ranging from a few nanometres to thousands of nanometres and can also be used to create multilayer coatings, deposits with graded compositions, thick deposits and freestanding structures. The substrates can range in size from very small to large, such as the glass panels used in architectural glass.

The thermal evaporation process was conducted to deposit a thin film on the low carbon steel specimens. The specimens were first cleaned and polished to remove any impurities. The tungsten boat was then loaded with the starting powder nanomaterials, which were weighed and placed in the centre of the vacuum chamber as shown in Figure 4(a). position process was carried out using thermal evaporation, a type of PVD method.



Fig. 4. (a) Tungsten boat (b) The thermal evaporation unit

The parameters used in the process are shown in Table 3. The thin film obtained after the deposition process was complete was reddish coppery to shiny coppery in colour and was uniform due to the prolonged time the coating material was evaporated. The deposition process consisted of various units, as depicted in Figure 4(b).

**Table 3**

Parameters for PVD of Cu-NP

PVD	Time (min)	Thickness (nm)	Power	Effective Pressure	Base pressure
Cu-NP	7	100	120A	$4 \times 10^5$ Pa	$4 \times 10^5$ Pa

### 2.4 X-Ray Diffraction (XRD)

XRD is a widely used non-destructive technique that enables the assessment of material's crystal structure. By comparing the acquired data with reference databases, XRD can identify crystalline phases and determine the chemical composition of the material. Its versatile applications include analysing minerals, polymers, corrosion products and unidentified substances. In typical scenarios, finely powdered samples undergo analysis through powder diffraction in XRD studies.

The XRD analysis works by exposing a sample to an x-ray beam, measuring the scattered intensity and determining the crystalline structure of the material based on the diffraction pattern produced. The Rietveld refinement approach is used to identify the most likely crystal structure responsible for

the observed pattern. XRD can be used in conjunction with a base metal to identify the presence of nanoparticle phases and structures. The device used in this case was a PHILIPS PW1730 model made in the Netherlands.

The measurement is based on Bragg's law in Eq. (1). Meanwhile the X-ray incident can be shown in Figure 5.

$$n\lambda = 2d \sin \theta \quad (1)$$

where,

$n$  = represents the order of diffraction,

$\lambda$  = the wavelength of incident X-ray.

$d$  = the spacing between the planes under consideration.

$\theta$  = Bragg's angle.

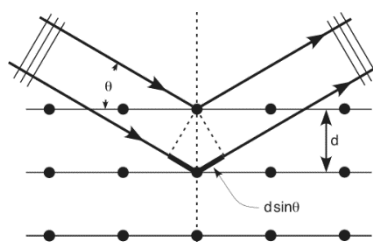


Fig. 5. Bragg's diffraction

### 2.5 Scanning Electron Microscopy (SEM)

SEM, a type of electron microscope, is commonly employed to investigate and quantify the surface morphology of a specimen. Electron microscopes are advanced scientific instruments capable of detailed analyses on a minuscule scale using high-energy electron beams. Through this analysis, valuable insights are gained regarding the sample's topography (surface characteristics), particle morphology (shape and size), elemental and compound composition, as well as crystallographic details (atomic arrangement). As the electron beam interacts with the sample, the resulting electron beam is influenced by these interactions, which are subsequently examined and presented visually.

SEM has a wide range of applications, including topographic studies, microstructure analysis and element analysis (when equipped with suitable detectors). Dispersive X-rays are used to analyse chemical structure and map elements. The FESEM machine used in this analysis was manufactured by the TESCAN company, model MIRA III and was made in the Czech Republic.

### 2.6 Transient Plane Source (TPS)

The Hot Disk TPS Thermal Constants Analysis [23] is an effective technique utilized for assessing the thermal characteristics of thin films, including conductivity, specific heat and diffusivity. Employing a TPS thin-film sensor, which comprises a double spiral nickel element with a thickness of 10 micrometres, sandwiched between two 25-micrometer thick Kapton layers using adhesive material [22], this method offers precise measurements. Following the TPS method for thin films [24], the sensor is positioned between two identical sections of the sample, supported by a background material. This equipment is specifically designed for accurate and reliable determination of the thermal properties of thin films.

### 3. Result and Discussion

In this results section, the physical properties of Cu-NP deposited on low carbon steel have been analysed and studied. The results of various tests, including XRD (XRD) and SEM, have been presented to gain a deeper understanding of the structural and morphological properties of the films. The data obtained from these studies will contribute to the development of new applications for Cu-NP in renewable energy and will provide a basis for future research in the field. Additionally, this section focuses on exploring ways to increase the thermal efficiency of the samples studied.

#### 3.1 Characterization Study

One of the environmentally friendly deposition techniques is the PVD-evaporation method. This method has gained significant attention due to its benefits, such as a high deposition rate, uniformity over large substrates and control over the composition and repeatability of deposited films [25]. The properties of the deposited thin films are affected by various process parameters such as vacuum conditions, deposition time, evaporation power and working pressure [26], which can alter the microstructure of the films. As we know, the physical and mechanical properties of the films are controlled by their microstructure [27].

XRD and field emission scanning electron microscopy (FESEM) analyses confirmed the formation of nanoscale structures (Cu-NP) on the low carbon steel substrate as shown in Figure 6. The evaporation process was conducted at a power of 120 A, an effective pressure of  $4 \times 10^5$  Pa and a deposition time of 7 minutes, all performed at room temperature. XRD analysis was performed on the sample to determine the possible phases present, including copper (Cu) and cupric oxide (CuO), as well as the size of the nanoparticles. Cupric oxide is a monoclinic semiconductor with a direct band gap range of 1.3-2.1 eV.



**Fig. 6.** The deposited film on the samples

#### 3.2 XRD Analysis

The XRD studies were conducted on two samples, sample 1 ( $S_1$ ) being the low carbon steel substrate before the deposition process and sample 2 ( $S_2$ ) being the low carbon steel substrate coated with copper through PVD-evaporation for 7 minutes at a power of 120A. XRD analyses were conducted in the  $2\theta$  range of  $4^\circ$  to  $80^\circ$ , with a scanning step size of 0.05. By employing the Scherrer equation in Eq. (2), the Cu-NP average crystallite size and the grain size of the low carbon steel substrate were determined based on the XRD patterns.

$$d = \frac{k\lambda}{\beta \cos(\theta)} \quad (2)$$

where the value of  $d$  represents the size of the crystallites,  $k$  is Scherrer constant ( $= 0.94$  assuming that the particles are spherical) and  $\lambda$ ,  $\theta$  and  $\beta$  are the wavelength of the X-ray radiation ( $1.541874 \text{ \AA}$ ), the Bragg diffraction angle and the full width of the peak at half maximum (FWHM), respectively.

Figure 7(a) shows the XRD pattern of low carbon steel before undergoing the PVD process, while Figure 7(b) displays the XRD pattern of the sample after the deposition process. The findings from the latter reveal the formation of copper and cupric oxide (CuO) due to the reduction in values between these two peaks. The first peak shows a value of 9850 and after deposition, this value decreases to 3500. The reaction between oxygen and copper in the chamber leads to the formation of a coating that consists of both copper (Cu) and cupric oxide (CuO) on the surface of the low carbon steel substrate. Despite using a copper target, the presence of oxygen in the chamber, even with the use of a vacuum pump, leads to the formation of copper oxide (CuO) phase. The increase in the  $O_2$  flow ratio results in an increase in the atomic O density in the plasma, leading to the formation of a cupric oxide (CuO) thin film [21].

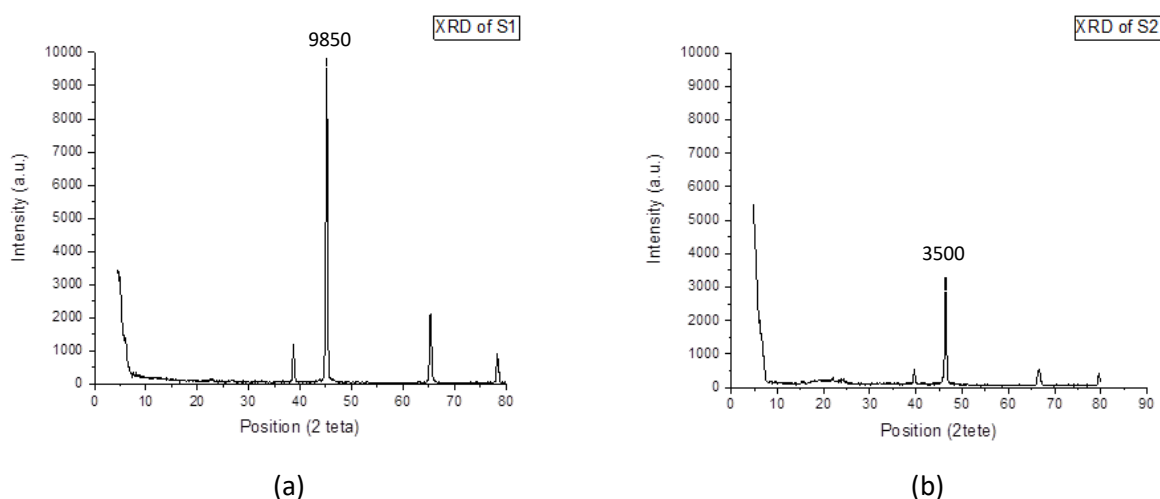


**Fig. 7.** XRD patterns of (a) low carbon steel sample (before deposition process,  $S_1$ ) (b) low carbon steel sample (after deposition of Cu-NP by PVD-evaporation method,  $S_2$ )

The XRD patterns of Cu nanoparticles, as compared to a copper standard (JCPDS 04-0836) in Figure 8, showed three reflections at  $2\theta$  angles of  $43.53^\circ$ ,  $50.5^\circ$  and  $74.23^\circ$ . These reflections were attributed to the (111), (200) and (220) crystal planes of the face centred cubic (FCC) structure, respectively. In addition, several peaks from impurity phases were detected, which were related to the presence of cupric oxide (CuO) due to the oxidation of copper particles evaporated from the copper target surface. Along with the peaks corresponding to the low carbon steel substrate, two XRD peaks at  $2\theta$  angles of  $35.77^\circ$  and  $38.68^\circ$  were observed, which were assigned to the diffraction from the (002) and (111) planes of CuO (JCPDS 48-1548) [11,21]. The average grain size of the Cu nanoparticles was estimated to be approximately 14 nm. These XRD results indicated that films with a mixture of Cu and CuO phases can be prepared and confirmed the generation of nanoscale crystals in the deposited films.



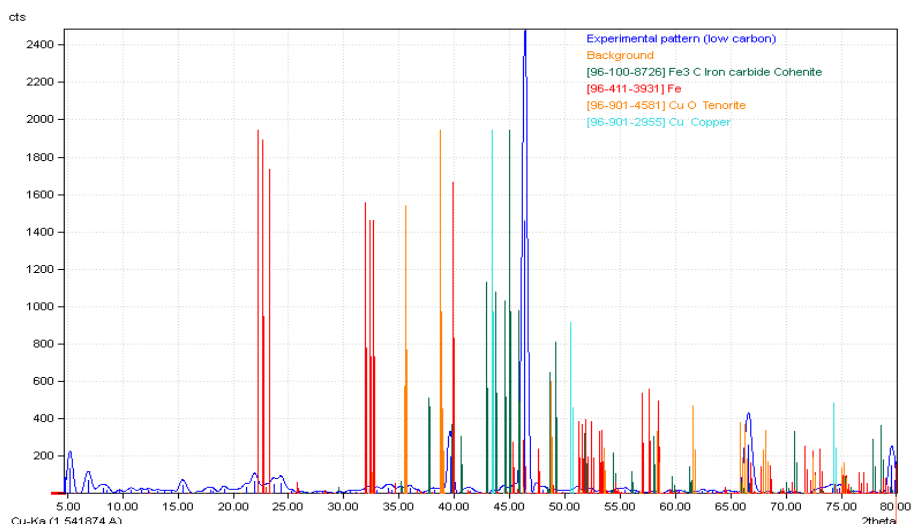


**Fig. 8.** Copper standard (JCPDS 04-0836) with the results of the experiment

### 3.3 Field Emission Scanning Electron Microscopy (FE-SEM) Analysis

The FESEM results showed the morphology and particle size distribution of the two samples,  $S_1$  (the low carbon steel substrate before deposition process) and  $S_2$  (the low carbon steel substrate after deposition of Cu-NP by PVD-evaporation method). The surface morphology of the two samples can be seen in Figure 9, where a magnification of 200,000x has been implemented. As seen in Figure 9(a), the low carbon steel substrate before deposition process ( $S_1$ ) has spherical grains with an average size of 50 nm. On the other hand, the FESEM image of the low carbon steel coated with Cu-NP by PVD-evaporation for 7 minutes at 120A ( $S_2$ ) is shown in Figure 9(b). This image demonstrates the presence of small, well-defined, homogeneously distributed Cu-NP with an average size of 20-25 nm to 140 nm on the low carbon steel surface, which confirms the formation of a copper coating through the PVD-evaporation process. The Cu-NP are observed as agglomerates of spherical and quasi-spherical shapes.

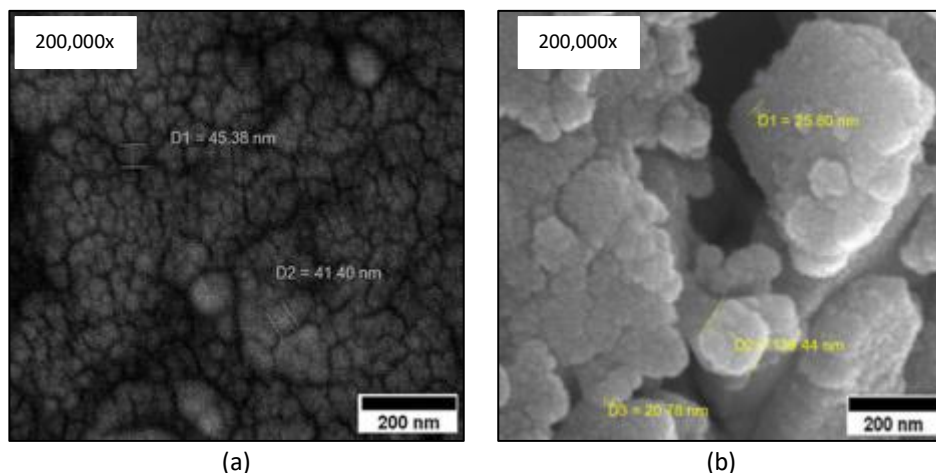


**Fig. 9.** FESEM images of (a) low carbon steel sample (before deposition process,  $S_1$ ) (b) low carbon steel sample (after deposition of Cu-NP by PVD-evaporation method,  $S_2$ )

### 3.4 Thermal Conductivity (Q)

It's is a measure of the capability of a material to conduct heat and we used Fourier's law of heat conduction as shown below in Eq. (3):

$$Q_{cond} = -KA\left(\frac{dt}{dx}\right) \quad (3)$$

where,

$K$  = Thermal conductivity

$A$  = area

$dT/dx$ = The slope of the temperature curve on a  $T$ - $x$  diagram.

Table 4 displays the results of the thermal conductivity tests for low carbon steel without PVD. After four tests was conducted, we obtain average around 49.662 W/ m·K, which was recorded for a sample taken from the low carbon steel.

**Table 4**  
 Thermal conductivity of low carbon steel before deposition

Measurement	T °C	K W/(m·K)	Error
1	27.67	49.800	0.0017
2	28.36	49.700	0.0102
3	28.97	49.650	0.0284
4	29.77	49.500	0.0204
Average		49.662	

It can be seen from the Table 5 that after using PVD techniques, the thermal conductivity of low carbon steel was improved and was found to be 50.1375 W/ m·K after taking the average of the four tests. Compared to Table 4, it was found that the thermal conductivity improved by 1%. This shows that the deposition of Cu-NP using PVD-evaporation method has a positive effect on the thermal conductivity of low carbon steel.

**Table 5**  
 Thermal conductivity test for low carbon steel + Cu-NP

Measurement	T °C	K W/(m·K)	Error	Operations
1	24.42	50.140	0.0103	evaporation
2	24.47	50.100	0.0102	evaporation
3	25.85	50.180	0.0101	evaporation
4	25.53	50.130	0.0105	evaporation
Average		50.1375		

## 4. Conclusion

The increasing demand for renewable energy has prompted scientists to concentrate on renewable energy sources as a research area. One of the most prominent of these sources is solar energy, which is clean, low-cost and free from harmful pollutants and can be converted into other forms of energy. The absorber surface is the central component of a solar thermal collector and its

role is to absorb sunlight and convert it into heat. In this study, the researchers used low carbon steel as the base material and deposited Cu-NP on it using PVD technology.

The results showed that depositing Cu-NP on low carbon steel has marginally increased the thermal conductivity by 1%. This improvement enhanced the performance of the solar thermal collector. The findings of this study have important implications for future research in this field. Although the increase in thermal conductivity is relatively small, it is important to bear in mind that this is only an early stage of the study and its performance can be further enhanced through other methods, such as multilayer deposition. This results also in line with Kabir *et al.*, [18] reported that the deposition of Cu-NP onto low carbon steel enhanced the material's light absorption and heat transfer capabilities, leading to improved overall efficiency. But they also exhibit a small improvement of efficiency about 1% to 2%. It is recommended that future studies explore the use of additional layers to protect increase the efficiency of thermal conductivity as well as protecting the surface from oxidizing agents and environmental conditions. It is also suggested to use tests such as UV to measure the reflection of rays falling on the surface and TEM examination to determine the thickness of the coating.

In conclusion, the increasing need for renewable energy sources has brought attention to solar energy and the absorber surface plays a crucial role in solar thermal collection. This study shows that coating low carbon steel with Cu-NP using PVD technology can improve thermal conductivity and enhance the performance of the solar thermal collector. Future research should focus on exploring additional ways to protect the surface and measuring the reflection and coating thickness.

### Acknowledgement

The research has been funded by the Ministry of Higher Education (MOHE) Malaysia, Malaysia under the Fundamental Research Grant Scheme with grant number FRGS/1/2020/TK0/UKM/03/1 and FRGS/1/2021/TK0/UKM/03/2. It is also partly funded by Universiti Kebangsaan Malaysia (UKM), Malaysia under the grant GGPM-2021-008.

### References

- [1] Mekhilef, Saidur, Rahman Saidur and Azadeh Safari. "A review on solar energy use in industries." *Renewable and sustainable energy reviews* 15, no. 4 (2011): 1777-1790. <https://doi.org/10.1016/j.rser.2010.12.018>
- [2] Suman, Siddharth, Mohd Kaleem Khan and Manabendra Pathak. "Performance enhancement of solar collectors—A review." *Renewable and Sustainable Energy Reviews* 49 (2015): 192-210. <https://doi.org/10.1016/j.rser.2015.04.087>
- [3] Farchado, M., J. M. Rodríguez, G. San Vicente, N. Germán and A. Morales. "Optical parameters of a novel competitive selective absorber for low temperature solar thermal applications." *Solar Energy Materials and Solar Cells* 178 (2018): 234-239. <https://doi.org/10.1016/j.solmat.2018.01.031>
- [4] Manikandan, G. K., S. Iniyan and Ranko Goic. "Enhancing the optical and thermal efficiency of a parabolic trough collector—A review." *Applied energy* 235 (2019): 1524-1540. <https://doi.org/10.1016/j.apenergy.2018.11.048>
- [5] Zhang, Hu, Yueming Li and Wenquan Tao. "Effect of radiative heat transfer on determining thermal conductivity of semi-transparent materials using transient plane source method." *Applied Thermal Engineering* 114 (2017): 337-345. <https://doi.org/10.1016/j.applthermaleng.2016.11.208>
- [6] Bozorgan, Navid and Maryam Shafahi. "Performance evaluation of nanofluids in solar energy: a review of the recent literature." *Micro and Nano Systems Letters* 3 (2015): 1-15. <https://doi.org/10.1186/s40486-015-0014-2>
- [7] Omeiza, Lukman Ahmed, Muhammad Abid, Yathavan Subramanian, Anitha Dhanasekaran, Saifullah Abu Bakar and Abul Kalam Azad. "Challenges, limitations and applications of nanofluids in solar thermal collectors—a comprehensive review." *Environmental Science and Pollution Research* (2023): 1-29. <https://doi.org/10.1007/s11356-023-30656-9>
- [8] Al-Abayechi, Yasir, Yaser Alaiwi and Zainab Al-Khafaji. "Exploration of key approaches to enhance evacuated tube solar collector efficiency." *Journal of Advanced Research in Numerical Heat Transfer* 19, no. 1 (2024): 1-14. <https://doi.org/10.37934/arnht.19.1.114>

- [9] Holleck, H. and V. Schier. "Multilayer PVD coatings for wear protection." *Surface and Coatings Technology* 76 (1995): 328-336. [https://doi.org/10.1016/0257-8972\(95\)02555-3](https://doi.org/10.1016/0257-8972(95)02555-3)
- [10] Ali, Abu Raihan Ibna and Bodius Salam. "A review on nanofluid: preparation, stability, thermophysical properties, heat transfer characteristics and application." *SN Applied Sciences* 2, no. 10 (2020): 1636. <https://doi.org/10.1007/s42452-020-03427-1>
- [11] Herrera-Zamora, D. M., F. I. Lizama-Tzec, I. Santos-González, R. A. Rodríguez-Carvajal, O. García-Valladares, O. Arés-Muzio and G. Oskam. "Electrodeposited black cobalt selective coatings for application in solar thermal collectors: Fabrication, characterization and stability." *Solar Energy* 207 (2020): 1132-1145. <https://doi.org/10.1016/j.solener.2020.07.042>
- [12] Kadhim, Mohammed J., Khalid A. Sukkar and Ahmed S. Abbas. "Copper Thin Film Deposited by PVD on Aluminum AA4015 substrate for thermal solar application." In *IOP Conference Series: Materials Science and Engineering*, vol. 518, no. 3, p. 032048. IOP Publishing, 2019. <https://doi.org/10.1088/1757-899X/518/3/032048>
- [13] Li, Zhong and Khiam Aik Khor. "Preparation and properties of coatings and thin films on metal implants." (2019): 203-212. <https://doi.org/10.1016/B978-0-12-801238-3.11025-6>
- [14] Lin, Yaxue, Yuting Jia, Guruprasad Alva and Guiyin Fang. "Review on thermal conductivity enhancement, thermal properties and applications of phase change materials in thermal energy storage." *Renewable and sustainable energy reviews* 82 (2018): 2730-2742. <https://doi.org/10.1016/j.rser.2017.10.002>
- [15] Simón-Allué, Raquel, Isabel Guedeá, Raúl Villén and Gonzalo Brun. "Experimental study of Phase Change Material influence on different models of Photovoltaic-Thermal collectors." *Solar Energy* 190 (2019): 1-9. <https://doi.org/10.1016/j.solener.2019.08.005>
- [16] Yang, Yuyi. "The study of nanostructured solar selective coatings." PhD diss., University of York, 2012.
- [17] Mello, Mario F., Eudes V. Santos, Marcos M. Falkembach, Cristina Pasqualli and Michele Siben. "The importance of using alternative energy sources within a new global perspective." In *New Global Perspectives on Industrial Engineering and Management: International Joint Conference ICIEOM-ADINGOR-IISE-AIM-ASEM*, pp. 21-29. Springer International Publishing, 2019. [https://doi.org/10.1007/978-3-319-93488-4\\_3](https://doi.org/10.1007/978-3-319-93488-4_3)
- [18] Kabir, Ehsanul, Pawan Kumar, Sandeep Kumar, Adedeji A. Adelodun and Ki-Hyun Kim. "Solar energy: Potential and future prospects." *Renewable and Sustainable Energy Reviews* 82 (2018): 894-900. <https://doi.org/10.1016/j.rser.2017.09.094>
- [19] Kennedy, Cheryl E. *Review of mid-to high-temperature solar selective absorber materials*. No. NREL/TP-520-31267. National Renewable Energy Lab.(NREL), Golden, CO (United States), 2002.
- [20] Suman, Siddharth, Mohd Kaleem Khan and Manabendra Pathak. "Performance enhancement of solar collectors— A review." *Renewable and Sustainable Energy Reviews* 49 (2015): 192-210. <https://doi.org/10.1016/j.rser.2015.04.087>
- [21] Shahabuddin, M., Mohammad A. Alim, Tanvir Alam, M. Mofijur, Shams F. Ahmed and Greg Perkins. "A critical review on the development and challenges of concentrated solar power technologies." *Sustainable Energy Technologies and Assessments* 47 (2021): 101434. <https://doi.org/10.1016/j.seta.2021.101434>
- [22] Pihl, Erik, Duncan Kushnir, Björn Sandén and Filip Johnsson. "Material constraints for concentrating solar thermal power." *Energy* 44, no. 1 (2012): 944-954. <https://doi.org/10.1016/j.energy.2012.04.057>
- [23] Xu, G., J. M. LaManna, J. T. Clement and M. M. Mench. "Direct measurement of through-plane thermal conductivity of partially saturated fuel cell diffusion media." *Journal of Power Sources* 256 (2014): 212-219. <https://doi.org/10.1016/j.jpowsour.2014.01.015>
- [24] Ahadi, Mohammad, Mehdi Andisheh-Tadbir, Mickey Tam and Majid Bahrami. "An improved transient plane source method for measuring thermal conductivity of thin films: Deconvoluting thermal contact resistance." *International Journal of Heat and Mass Transfer* 96 (2016): 371-380. <https://doi.org/10.1016/j.ijheatmasstransfer.2016.01.037>
- [25] Liu, Yiming, Jianjun Zhang, Wanggang Zhang, Wei Liang, Bin Yu and Jinbo Xue. "Effects of annealing temperature on the properties of copper films prepared by magnetron sputtering." *Journal of Wuhan University of Technology-Mater. Sci. Ed.* 30, no. 1 (2015): 92-96. <https://doi.org/10.1007/s11595-015-1106-9>
- [26] Nayan, Nafarizal, Mohd Zainizan Sahdan, Low Jia Wei, Mohd Khairul Ahmad, Jais Lias, Ali Yeon Md Shakaff, Ammar Zakaria and Ahmad Faizal Mohd Zain. "Sputter deposition of cuprous and cupric oxide thin films monitored by optical emission spectroscopy for gas sensing applications." *Procedia Chemistry* 20 (2016): 124-129. <https://doi.org/10.1016/j.proche.2016.07.023>
- [27] Zhuang, Yan-Xin, Xiu-Lan Zhang and Xian-Yu Gu. "Effect of annealing on microstructure and mechanical properties of Al<sub>0.5</sub>CoCrFeMoxNi high-entropy alloys." *Entropy* 20, no. 11 (2018): 812. <https://doi.org/10.3390/e20110812>